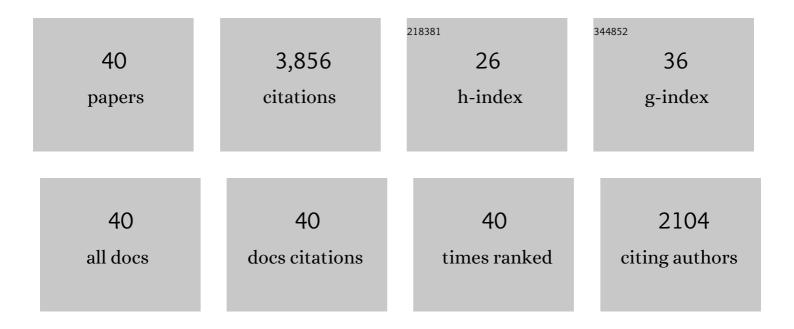
T Irifune

List of Publications by Year in descending order

Source: https://exaly.com/author-pdf/10784077/publications.pdf Version: 2024-02-01



TIDIELINE

#	Article	IF	CITATIONS
1	Phase transformations in subducted oceanic crust and buoyancy relationships at depths of 600–800 km in the mantle. Earth and Planetary Science Letters, 1993, 117, 101-110.	1.8	418
2	Nature of the 650–km seismic discontinuity: implications for mantle dynamics and differentiation. Nature, 1988, 331, 131-136.	13.7	295
3	Experimental determination of element partitioning between silicate perovskites, garnets and liquids: constraints on early differentiation of the mantle. Earth and Planetary Science Letters, 1988, 89, 123-145.	1.8	267
4	Subduction of continental crust and terrigenous and pelagic sediments: an experimental study. Earth and Planetary Science Letters, 1994, 126, 351-368.	1.8	264
5	Stability of hydrous silicate at high pressures and water transport to the deep lower mantle. Nature Geoscience, 2014, 7, 224-227.	5.4	259
6	The Postspinel Phase Boundary in Mg2SiO4 Determined by in Situ X-ray Diffraction. Science, 1998, 279, 1698-1700.	6.0	251
7	The eclogite-garnetite transformation at high pressure and some geophysical implications. Earth and Planetary Science Letters, 1986, 77, 245-256.	1.8	225
8	Phase transformations in a harzburgite composition to 26 GPa: implications for dynamical behaviour of the subducting slab. Earth and Planetary Science Letters, 1987, 86, 365-376.	1.8	214
9	A new high-pressure form of MgAl2O4. Nature, 1991, 349, 409-411.	13.7	214
10	Hardness and deformation microstructures of nano-polycrystalline diamonds synthesized from various carbons under high pressure and high temperature. Journal of Materials Research, 2007, 22, 2345-2351.	1.2	168
11	Phase relations and equations of state ofZrO2under high temperature and high pressure. Physical Review B, 2001, 63, .	1.1	140
12	Sound velocities of majorite garnet and the composition of the mantle transition region. Nature, 2008, 451, 814-817.	13.7	130
13	Microstructure features of polycrystalline diamond synthesized directly from graphite under static high pressure. Journal of Materials Science, 2004, 39, 445-450.	1.7	112
14	Indentation hardness of nano-polycrystalline diamond prepared from graphite by direct conversion. Diamond and Related Materials, 2004, 13, 1771-1776.	1.8	109
15	Constraints on element partition coefficients between MgSiO3 perovskite and liquid determined by direct measurements. Earth and Planetary Science Letters, 1988, 90, 65-68.	1.8	96
16	In situ X-ray observations of phase transitions in MgAl 2 O 4 spinel to 40 GPa using multianvil apparatus with sintered diamond anvils. Physics and Chemistry of Minerals, 2002, 29, 645-654.	0.3	68
17	Conditions and mechanism of formation of nano-polycrystalline diamonds on direct transformation from graphite and non-graphitic carbon at high pressure and temperature. High Pressure Research, 2006, 26, 63-69.	0.4	68
18	The phase boundary between wadsleyite and ringwoodite in Mg2SiO4 determined by in situ X-ray diffraction. Physics and Chemistry of Minerals, 2006, 33, 106-114.	0.3	58

T Irifune

#	Article	IF	CITATIONS
19	Pressure-induced nano-crystallization of silicate garnets from glass. Nature Communications, 2016, 7, 13753.	5.8	53
20	Determination of the phase boundary between ilmenite and perovskite in MgSiO 3 by in situ X-ray diffraction and quench experiments. Physics and Chemistry of Minerals, 2000, 27, 523-532.	0.3	44
21	High-pressure phase transformation in CaMgSi2O6and implications for origin of ultra-deep diamond inclusions. Geophysical Research Letters, 2000, 27, 3541-3544.	1.5	38
22	Application of synchrotron radiation and Kawai-type apparatus to various studies in high-pressure mineral physics. Mineralogical Magazine, 2002, 66, 769-790.	0.6	37
23	Crystal chemistry of dense hydrous magnesium silicates: The structure of phase H, MgSiH2O4, synthesized at 45 GPa and 1000 ÂC. American Mineralogist, 2014, 99, 1802-1805.	0.9	36
24	Ultrahard diamond indenter prepared from nanopolycrystalline diamond. Review of Scientific Instruments, 2008, 79, 056102.	0.6	31
25	Mineralogy of the Earth $\hat{a} \in $ Phase Transitions and Mineralogy of the Lower Mantle. , 2007, , 33-62.		30
26	Phase relations and formation of chromium-rich phases in the system Mg4Si4O12–Mg3Cr2Si3O12 at 10–24 GPa and 1,600°C. Contributions To Mineralogy and Petrology, 2015, 169, 1.	1.2	28
27	Note: High-pressure generation using nano-polycrystalline diamonds as anvil materials. Review of Scientific Instruments, 2011, 82, 066104.	0.6	27
28	Phase Transitions and Mineralogy of the Lower Mantle. , 2015, , 33-60.		26
29	Mineralogy of the Earth $\hat{a} \in $ Phase Transitions and Mineralogy of the Lower Mantle. , 2007, , 33-62.		25
30	In situ stress-strain measurements in a deformation-DIA apparatus at P-T conditions of the upper part of the mantle transition zone. American Mineralogist, 2011, 96, 1665-1672.	0.9	23
31	High-temperature and high-pressure equation of state for the hexagonal phase in the system NaAlSiO4 – MgAl2O4. Physics and Chemistry of Minerals, 2005, 32, 594-602.	0.3	22
32	Solid Solution and Compression Behavior of Hydroxides in the Lower Mantle. Journal of Geophysical Research: Solid Earth, 2019, 124, 10231-10239.	1.4	16
33	In situ X-ray diffraction study of an aluminous phase in MORB under lower mantle conditions. Physics and Chemistry of Minerals, 2006, 33, 28-34.	0.3	14
34	Phase transitions of serpentine in the lower mantle. Physics of the Earth and Planetary Interiors, 2015, 245, 52-58.	0.7	14
35	Nano-polycrystalline diamond anvils: key devices for XAS at extreme conditions: their use, scientific impact, present status and future needs. High Pressure Research, 2020, 40, 65-81.	0.4	13
36	Constraints on element partition coefficients between MgSiO3 perovskite and liquid determined by direct measurements—reply to C.B. Agee and D. Walker. Earth and Planetary Science Letters, 1989, 94, 162-164.	1.8	10

T Irifune

#	Article	IF	CITATIONS
37	Laser heating in nano-polycrystalline diamond anvil cell. Journal of Physics: Conference Series, 2010, 215, 012192.	0.3	7
38	Phase Relations in the Model System SiO2–MgO–Cr2O3: Evidence from the Results of Experiments in Petrologically Significant Sections at 12–24 GPa and 1600°C. Petrology, 2018, 26, 588-598.	0.2	3
39	Chemical Reaction Between Metallic Iron and a Limited Water Supply Under Pressure: Implications for Water Behavior at the Coreâ€Mantle Boundary. Geophysical Research Letters, 2020, 47, e2020GL089616.	1.5	3
40	Grain size dependent high-pressure elastic properties of ultrafine micro/nanocrystalline grossular. Scientific Reports, 2021, 11, 22481.	1.6	0